Phosphoproteomic profiling highlights CDC42 and CDK2 as key players in the regulation of the TGF-β pathway in *ALMS1* and *BBS1* knockout models

Brais Bea-Mascato[1,2], Girolamo Giudice[3], Iguaracy Pinheiro-de-Sousa[3], Carlos Solarat [1,2], Evangelia Petsalaki[3], Diana Valverde[1,2]

[1] CINBIO, Universidad de Vigo, 36310 Vigo, Spain.

[2] Grupo de Investigación en Enfermedades Raras y Medicina Pediátrica, Instituto de Investigación Sanitaria Galicia Sur (IIS Galicia Sur), SERGAS-UVIGO, Vigo, Spain

[3] European Molecular Biology Laboratory-European Bioinformatics Institute, Wellcome Genome Campus, Hinxton CB10 1SD, UK

Correspondence: Diana Valverde

CINBIO Facultad de Biología, Universidad de Vigo, Campus As Lagoas-Marcosende s/n, 36310 Vigo, Spain

Tel +34 986 811 953

Email: dianaval@uvigo.es

ABSTRACT

BACKGROUND

The primary cilium is a sensory organelle that extends from the plasma membrane. It plays a vital role in physiological and developmental processes by controlling different signalling pathways such as WNT, Sonic hedgehog (SHh), and transforming growth factor β (TGF-β). Ciliary dysfunction has been related to different pathologies such as Alström (ALMS) or Bardet-Biedl (BBS) syndrome. The leading cause of death in adults with these syndromes is chronic kidney disease (CKD), which is characterised by fibrotic and inflammatory processes often involving the TGF-β pathway.

METHODS

Using genomic editing with CRISPR-CAS9 and phosphoproteomics we have studied the TGF-β signalling pathway in knockout (KO) models for *ALMS1* and *BBS1* genes. We have developed a network diffusion-based analysis pipeline to expand the data initially obtained and to be able to determine which processes were deregulated in TGF-β pathway. Finally, we have analysed protein-protein and kinase-substrate interactions to prioritise candidate genes in the regulation of the TGF-β pathway in ALMS and BBS.

RESULTS

Analysis of differentially phosphorylated proteins identified 10 candidate proteins in the *ALMS1* KO model and 41 in the *BBS1* KO model. After network expansion using a random walk with a restart algorithm, we were able to identify the TGF-β signalling pathway together with other related processes such as endocytosis in the case of *ALMS1* or the regulation of the extracellular matrix in *BBS1*. Protein interaction analyses demonstrated the involvement of CDC42 as a central protein in the interactome in *ALMS1* and CDK2 in the case of *BBS1*.

CONCLUSION

In conclusion, the depletion of *ALMS1* and *BBS1* affects the TGF-β signalling pathway, conditioning the phosphorylation and activation of several proteins, including CDC42 in the case of *ALMS1* and CDK2 in the case of *BBS1*.

KEYWORDS: ALMS1, BBS1, ciliopathies, TGF-β, phosphoproteomics, Alström syndrome, Bardet-Biedl syndrome.

INTRODUCTION

The primary cilium is a microtubule-based sensory organelle that extends from the plasma membrane. It is present in all cell types and plays a vital role in physiological and developmental processes by controlling different signalling pathways such as WNT, Sonic hedgehog (SHh), and transforming growth factor β (TGF-β) (Berbari et al., 2009; Ishikawa and Marshall, 2011; Christensen et al., 2012; May-Simera et al., 2018; Anvarian et al., 2019). Ciliary dysfunction generates different phenotypes, the most common of which are obesity, type 2 diabetes mellitus, retinopathies or the appearance of multi-organ fibrosis leading to liver, kidney, or lung dysfunction (Gerdes et al., 2009; Waters and Beales, 2011; Reiter and Leroux, 2017; May-Simera et al., 2018).

The group of diseases characterised by ciliary dysfunction, mutations in primary cilium or basal body genes, are commonly known as ciliopathies. Alström syndrome (ALMS) and Bardet-Biedl syndrome (BBS) are two model ciliopathies where, despite the progress made in recent years, a clear pathological mechanism has not yet been established. (Forsythe and Beales, 2012; Forsythe et al., 2018; Hearn, 2018). ALMS is a monogenic recessive disease with an incidence of 1 in 1,000,000 individuals in the general population. To date, the only known causative gene is the *ALMS1* gene, which codes for a centrosome-associated protein, responsible for maintaining cohesion between the mother centriole and the daughter centriole (Collin et al., 2002; Hearn et al., 2005; Marshall et al., 2011). On the other hand, BBS is also an autosomal recessive disorder, with 23 causative genes described to date, named from *BBS1* to *BBS23*, being BBS1 the most prevalent gene with pathogenic variants in 23% of described cases (Forsythe and Beales, 2012; Forsythe et al., 2018; Perea-Romero et al., 2022). The main proteins of BBS, BBS1, BBS2, BBS4, BBS5, BBS7, BBS8, BBS9 and BBS18/BBSIP1, encode for an octameric protein complex called the BBSome involved in primary cilia transport (IFT), retrograde and anterograde (Klink et al., 2020; Singh et al., 2020). The clinical phenotypes of these two ciliopathies are overlapping, making their differentiation difficult and complicating the correct diagnosis (Aliferis et al., 2012). One of the main causes of death in adult patients with these syndromes is chronic kidney disease (CDK) (Li et al., 2007; Marshall et al., 2011; Putoux et al., 2012; Jaykumar et al., 2018; Waldman et al., 2018; Baig et al., 2020; Meyer et al., 2022). This disease is usually accompanied by

79 inflammatory and fibrotic processes that progressively degrade normal kidney function
80 until eventually renal failure and death occur (Meng et al., 2014).

81 The TGF-β pathway is one of the main pathways involved in fibrotic and inflammatory
82 processes at the cellular level (Lan, 2011; Finnson et al., 2020). It is related to the control
83 of several processes such as mitosis, apoptosis, cell migration or autophagy through
84 cross-signalling with other pathways such as MAPK, PI3K/AKT or SMADs (Massagué,
85 2012; Hamidi et al., 2017; Luo, 2017; Zhang et al., 2017; Gasior et al., 2019). In previous
86 studies in our laboratory, we have determined that *ALMS1* depletion leads to altered
87 signal transduction of the TGF-β pathway and other related pathways such as AKT or
88 p53 (Álvarez-Satta et al., 2021; Bea-Mascato et al., 2022b, 2022a), altering processes
89 such as cell migration or EMT. In this study, we apply an original approach based on
90 phosphoproteomics to delve into the regulation of the TGF-β pathway in ALMS and to
91 determine for the first time whether there are alterations in this pathway in BBS.

MATERIALS AND METHODS

Cell culture and CRISPR knockouts

The hTERT-BJ-5ta cell line, provided by the American Type Culture Collection (ATCC), was maintained in a medium composed of 4:1 of Dulbecco's minimal essential medium (DMEM, Gibco, Invitrogen, NY, USA) and Medium 199, Earle's Salts (Gibco, Invitrogen, NY, USA), supplemented with 10% fetal bovine serum (FBS) (Gibco, Invitrogen, NY, USA) and 2% penicillin/streptomycin (P/S) (Gibco, Invitrogen, NY, USA). In this study, a knockout model for the *BBS1* gene was generated **(Figure S1 A, B)** using 4 different sgRNAs **(Supplementary Table S1-2)** and a knockout (KO) model for the *ALMS1* gene previously generated in Bea-Mascato et al (Bea-Mascato et al., 2022b) was used. The methodology used in the generation of the *BBS1* model was the same as described in Bea-Mascato et al (Bea-Mascato et al., 2022b).

TGF-β stimulation and protein extraction

Cell lines were cultured in 150 mm dishes (Corning, NY, USA) until 90% confluence was reached and then serum starved for 24 hours. The following day, rhTGF-β1 ligand (R&D Systems; 240-B) was added to the plates at a final well concentration of 2ng/mL for 0 and 30 min. The plates were then washed 3 times with PBS and the cells were harvested in a volume of 1.5mL of PBS. They were then pelleted at 10000 rpm for 5 minutes in a Sigma® 1-14 K at 4°C. The PBS volume was removed from the tubes and the pellets were frozen at -80C until the experiment was continued.

Protein extraction was performed by adding 500µL of TEAB 100mM lysis buffer with 1% SDS (Thermo Fisher, Waltham, USA) to each sample. Samples were sonicated by giving five 5-second pulse intervals with a wave amplitude of 20% on a Branson ultra sonicator model 102C (Branson Ultrasonic, Connecticut, USA). They were then left to stand on ice for 10 minutes with moderate agitation. Finally, the cell debris was removed by centrifuging the samples for 30 minutes at 12000rpms in a Sigma® 1-14 K at 4°C. The supernatant from the tubes was transferred to low-binding tubes (Thermo Fisher, Waltham, USA) and stored at -80 degrees until the next step of the analysis.

120 Quantification of protein lysates was performed using the Pierce™ BCA Protein Assay Kit
121 (Thermo Fisher, Waltham, USA).

122 Reduction, alkylation and precipitation

123 Initially, samples were centrifuged at 16,000 rpm for 10 min at 4°C. Then, 600µg per
124 sample was transferred into a new 1.5 mL tube and adjusted to a final volume of 600µL
125 with 100mM TEAB buffer. Samples were divided into several tubes (200µL/tube). 10µL
126 of 200mM TCEP was added to each tube and incubated at 55°C for 1 hour. Then, 10µL
127 of 375mM iodoacetamide (IAA) was also added to the sample and incubated for 30
128 minutes protected from light at room temperature (RT). Finally, 6 volumes (1200µL) of
129 acetone pre-cooled to -20 degrees were added and left to precipitate overnight. The
130 next day the samples were centrifuged at 8000rpms for 12 min at 4°C, the acetone was
131 decanted off and the pellet was left to dry for 2-3 min.

132 Protein digestion and cleaning, TiO_2 enrichment, 133 TMT labelling and LC-MS/MS analysis

134 Approximately 200µg of protein pellets precipitated in acetone were resuspended with
135 200 µL of 100mM TEAB buffer. Then 5µL (5µg) of trypsin was added per tube and
136 digested at 37°C overnight. The next day, 10 µL of 5% trifluoroacetic acid (TFA) was
137 added to reduce the pH of the solution. Finally, peptide samples were cleaned up using
138 C18 desalting tips (Agilent OMIX 100 µL, SPE with pipette) and the pooled eluents with
139 speed-vac at 45°C. Phosphopeptide enrichment was performed using TiO_2 spin tips from
140 the High-SelectTM TiO_2 Phosphopeptide Enrichment Kit following the manufacturer's
141 protocol (Thermo Fisher, Waltham, USA). After enrichment, a further cleaning was
142 performed using C18 desalting tips.

143 Samples were resuspended in 50 µL of 100mM TEAB buffer and 20 µL of TMT label
144 reagent was added to each sample, using TMT10plex™ Isobaric Mass Tagging Kit
145 (Thermo Fisher, Waltham, USA). Samples were multiplexed and analyzed by LC-MS/MS
146 using a 90-minute gradient on Orbitrap Eclipse (Thermo Fisher, Waltham, USA) with a
147 method using CID-MSA for the identification of MS2 and a real-time search algorithm to
148 quantify reporters in MS3. As a quality control, the BSA controls were digested in parallel

149 and ran between each of their samples to avoid carryover and assess instrument
150 performance.

151 Protein identification and differential 152 phosphorylation analysis

153 The identification of peptides/proteins was performed using the software Proteome
154 Discoverer software (v2.5) **(Supplementary Table S3-4)**. Samples were searched against
155 the SP_Human database (March 2021), using the search algorithm Mascot v2.6
156 (http://www.matrixscience.com/). Peptides have been filtered based on false discovery
157 rate (FDR) and only peptides showing an FDR lower than 5% have been retained. The
158 peptides were grouped into proteins with the default option of Proteome discovery
159 (v2.5) and these were used in the downstream analysis.

160 The proteins resulting from the identification were used for differential phosphorylation
161 analysis. Each multiplexed/batch (with and without stimulation of the TGF-β pathway)
162 was analysed individually with the R (v4.2.1) package DEP (Zhang et al., 2018). The data
163 was filtered to keep only the proteins that were quantified in all samples of at least one
164 condition. Subsequently, the normalization of the data by variance stabilizing
165 normalization (VSN) was performed. Finally, for data imputation, the MiniProb
166 algorithm was used with a q-value of 0.01. The log2 fold change (FC) of the differentially
167 phosphorylated proteins was calculated against the controls (WT) of the corresponding
168 batch for both knockouts (*ALMS1* and *BBS1*) **(Supplementary Table S5-6)**. For
169 downstream analyses, the differentially phosphorylated protein was that with a value
170 of $|\log2FC| > 0.5$ and an $FDR < 0.05$.

171 Network diffusion, enrichment analysis and protein-172 protein interaction analysis:

173 For network diffusion analysis, a graph covering the entire human signalome was
174 created with the R package, igraph (Csardi and Nepusz, 2006). The creation of the human
175 interactome was performed as follows. Initially, the human interactome was extracted
176 from the IntAct database (version: 4.2.17, last updated May 2021) (Orchard et al., 2014).

177 In addition, kinase-substrate interactions and kinase-kinase interactions contained in
178 PhosphoSitePlus (Orchard et al., 2014) (version 6.5.9.3, last update May 2021),
179 OmniPath (Türei et al., 2016) (last version May 2021) and SIGNOR 2.0 (Licata et al., 2020)
180 (last version May 2021) were integrated in this interactome. All proteins not annotated
181 in Swiss-Prot (UniProt, 2021) and those not annotated with at least one GO term (Gene
182 Ontology, 2021) were removed. The resulting protein interaction network (PIN)
183 comprised a total of 16,407 nodes and 238,035 edges. The weight of edges was defined
184 by the semantic similarity between gene pairs, modelled according to Topological
185 Clustering Semantic Similarity (TCSS) algorithm (Jain and Bader, 2010) and calculated
186 using the Semantic Measure Library (Harispe et al., 2014). The raw PIN was normalised
187 to avoid hub bias using "correct.for.hubs" option in diffusR.

188 The differentially phosphorylated proteins detected in the "*Protein identification and*
189 *differential phosphorylation analysis*" section, were used as seed nodes in the
190 interactome graph. These nodes were assigned the same weight and a weight of 0 to
191 the rest of the network. Finally, the random walk with restart (RWR) algorithm (Tong et
192 al., 2006; Köhler et al., 2008) was used through the R package diffusR using a restart
193 probability of 0.3, 10,000 iterations and a threshold of 1e-06. Nodes were sorted by RWR
194 score after diffusion, and to ensure at least 10% real (not inferred) data, the top 100
195 were used in subsequent analyses **(Supplementary Table S7-8)**.

196 The enrichment analysis was performed using the R package enrichR, an R interface for
197 accessing the enrichR database (Kuleshov et al., 2016). The differentially phosphorylated
198 proteins and the 100 nodes with the highest RWR scores were compared with the GO
199 Molecular Function 2021, GO Biological Process 2021 and BioPlanet 2019 datasets in
200 independent enrichment analysis. Only the 20 processes with the lowest FDR were
201 considered using an FDR < 0.05 as a threshold.

202 The protein-protein interaction results obtained after network diffusion for the top 100
203 proteins was visualised with the help of Cytoscape software (v 3.9.1) (Shannon et al.,
204 2003).

205 Lastly, a kinase-substrate enrichment analysis (KSEA) was performed using the KEA3
206 web application (Kuleshov et al., 2021). The 100 proteins with the highest RWR score

were used as input. Both rows and columns of the graph were clustered using rank by sum to obtain the top substrate and top kinase in the first row and column of the heatmap.

RESULTS

ALMS1 and *BBS1* depletion alters the phosphorylation of several proteins upon TGF-β1 ligand stimulation

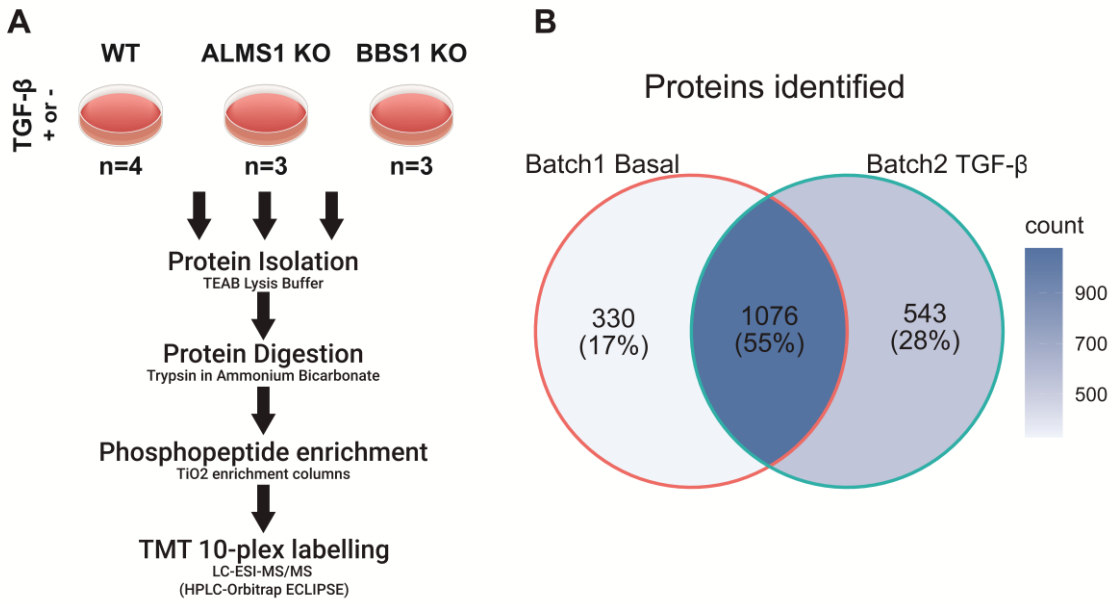

Figure 1. Experimental design of the phosphoproteome in basal and TGF-β-stimulated BJ-5ta. **(A)** Protocol followed for the generation of the phosphoproteomic datasets **(B)** Overlap between the proteins identified in Batch 1 (Basal) and Batch 2 (TGF-β).

To identify whether TGF-beta signalling was affected in the ALMS1 and BBS1 knockout cells and discover potentially new processes, we performed global phosphoproteomics in the presence and absence of TGF-β1 stimulation **(methods)**. The experiment was designed using two multiplexes of 10 samples each. The batch 1 contains all samples without TGF-β1 stimulation, while batch 2 contains all samples stimulated for 30 minutes with TGF-β1 **(Figure 1A-B)**. We identified a total of 2,720 phosphopeptides (1,406 proteins) in batch 1 (samples without stimulation) and 3,317 phosphopeptides (1,619 proteins) in batch 2 (samples with stimulation), 1076 common proteins were identified in both batches **(Figure 1B)**. Of the total peptides/proteins identified, 50-60%

227 were quantified in all samples of at least one condition (731 proteins in batch 1 and 960
228 in batch 2) **(Figure S1 C-F)**.

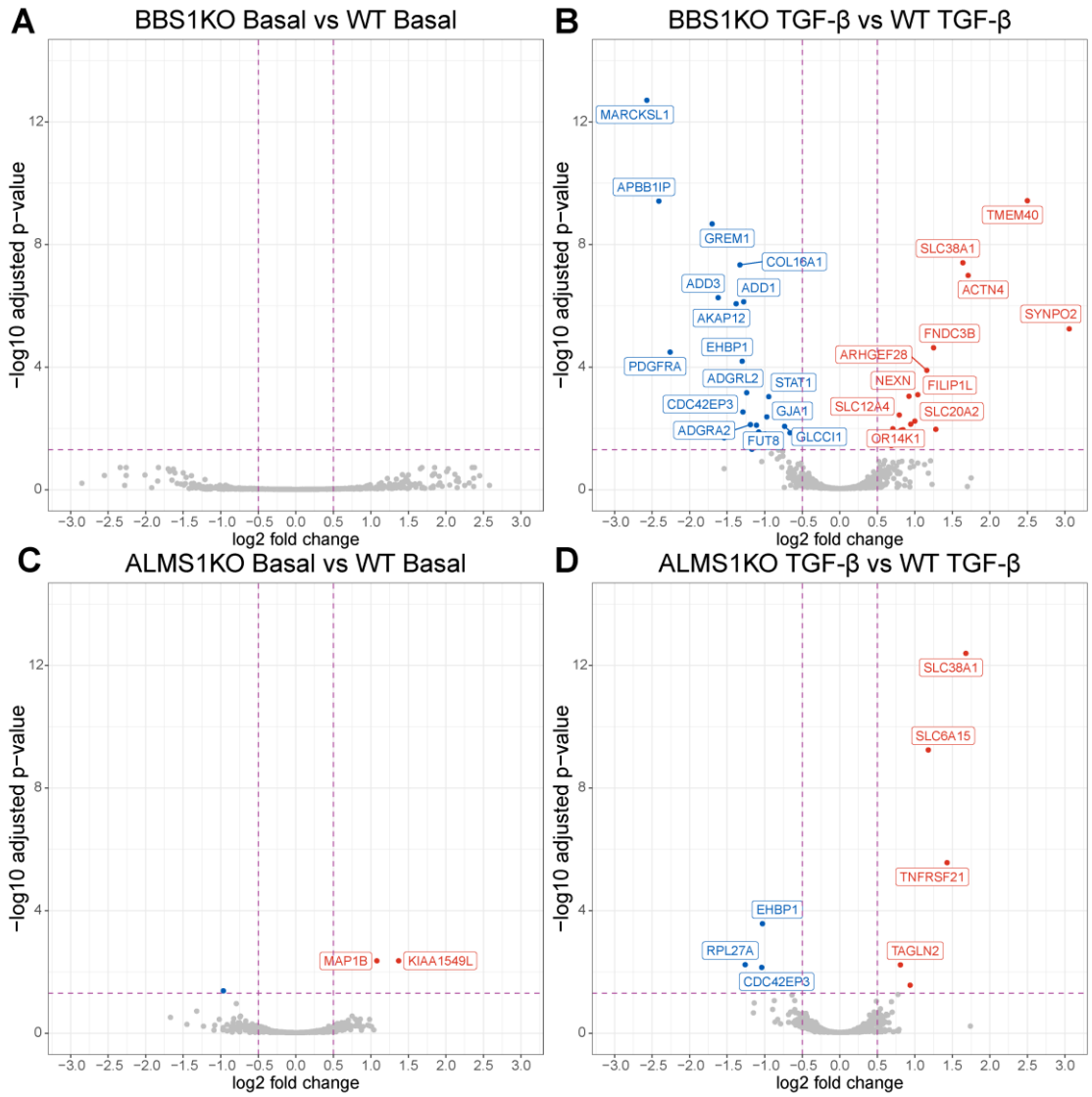

229

230 **Figure 2.** Differential phosphorylation analysis showed alterations in protein activation
231 after TGF-β stimulation. Labelled proteins have an FDR < 0.01. **(A)** Volcano-plot of
232 differentially phosphorylated proteins (DPP; FDR < 0.05) in *BBS1* knockout before TGF-β
233 stimulation **(B)** Volcano-plot of DPP in *BBS1* knockout after TGF-β stimulation **(C)**
234 Volcano-plot of DPP in *ALMS1* knockout before TGF-β stimulation **(D)** Volcano-plot of
235 DPP in *ALMS1* knockout after TGF-β stimulation.

236 After differential phosphorylation analysis, no significant proteins were detected in
237 batch 1 for *BBS1* knockout (BBS1KO) and 3 differentially phosphorylated proteins (DPP)
238 were detected in the case of *ALMS1* knockout (ALMS1KO) **(Figure 2A-C)**. Results from

239 batch 2 showed 41 DPP in BBS1KO and 10 in ALMS1KO **(Figure 2B-D)**. Of the total DPPs
240 detected in the cell models, 4 were common among them, 3 of them were infra-
241 phosphorylated (EHBP1, CDC42EP3, RPL27A) while 1 (SLC38A1) was over-
242 phosphorylated.

243 Network diffusion highlights the involvement of 244 *ALMS1* and *BBS1* in processes coordinated by the 245 TGF-β pathway

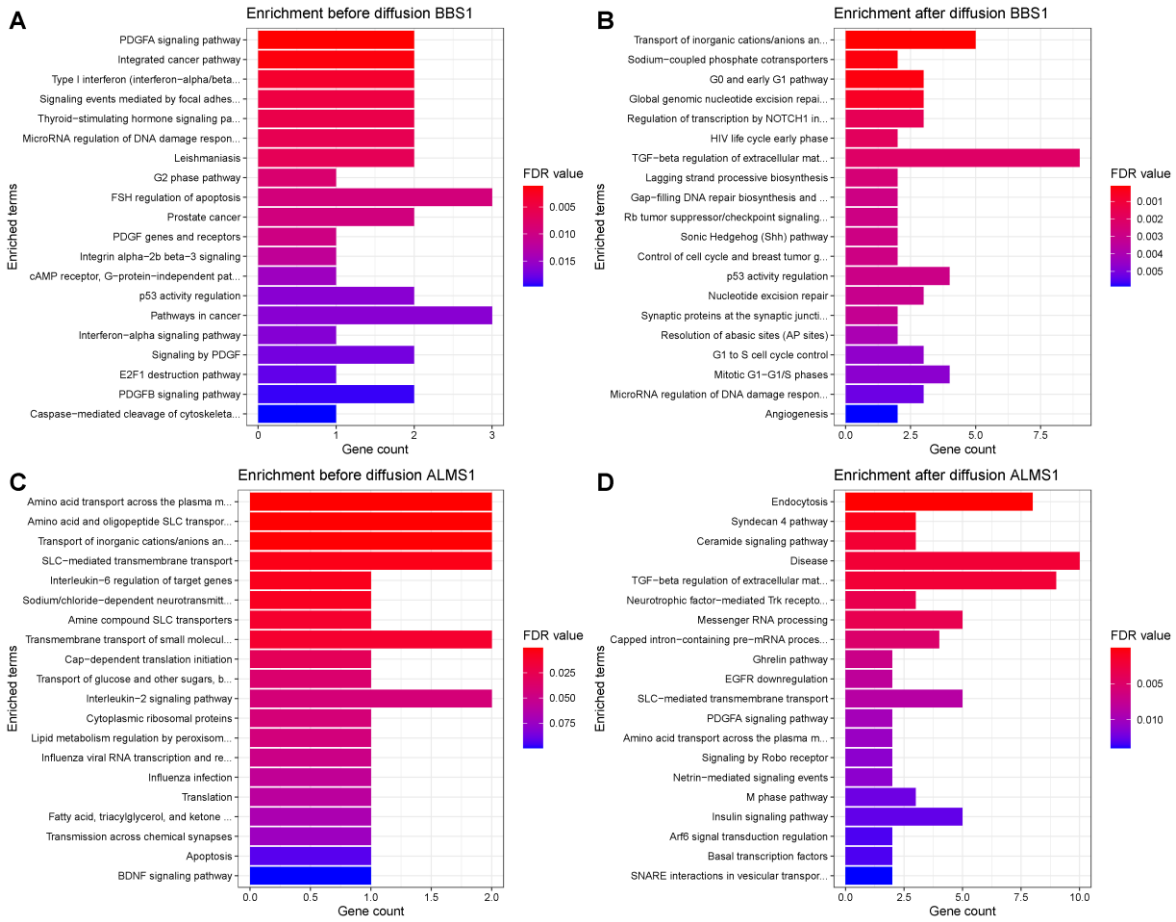

246

247 **Figure 3.** Over-representation analysis (ORA) after network diffusion reveals processes
248 controlled by TGF-β such as endocytosis, mitosis, or extracellular matrix in Bioplanet DB.
249 **(A)** ORA of DPP in the *BBS1*KO before network diffusion. **(B)** ORA of top 100 proteins
250 with the highest RWR score in the *BBS1*KO after network diffusion. **(C)** ORA of DPP in the
251 *ALMS1*KO before network diffusion. **(D)** ORA of top 100 proteins with the highest RWR
252 score in the *ALMS1*KO after network diffusion.

Then, we performed a pathway enrichment analysis **(methods)** to identify the processes that are most affected by *ALMS1* and *BBS1* depletion after TGF-β stimulation **(Figure 3)**. Pre-diffusion ORA was performed using the DPP after TGF-β stimulation (only seed nodes). Due to the small number of proteins and the low signal-to-noise ratio of phosphoproteomics, we were unable to identify the TGF-β pathway, which serves as a control of the analysis **(Figure 3A, C)**. To improve the signal-to-noise ration from our DPP, we applied a network diffusion-based analysis **(methods)**. The ORA after diffusion was performed with the top 100 proteins with the highest RWR score **(Figure 3B, D)**. In this case, we obtained TGF-β in both KO cell models. In addition, processes related to TGF-β regulation such as mitosis, NOTHC1, p53 or SHh signalling in the case of *BBS1KO* and endocytosis or Syndecan4 in the case of *ALMS1KO* were also identified **(Figure 3B, D)**.

Analysis of protein-protein interactions involves CDC42 and several RAB proteins in the alterations of TGF-β signalling in *ALMS1* and CDK2 in *BBS1*

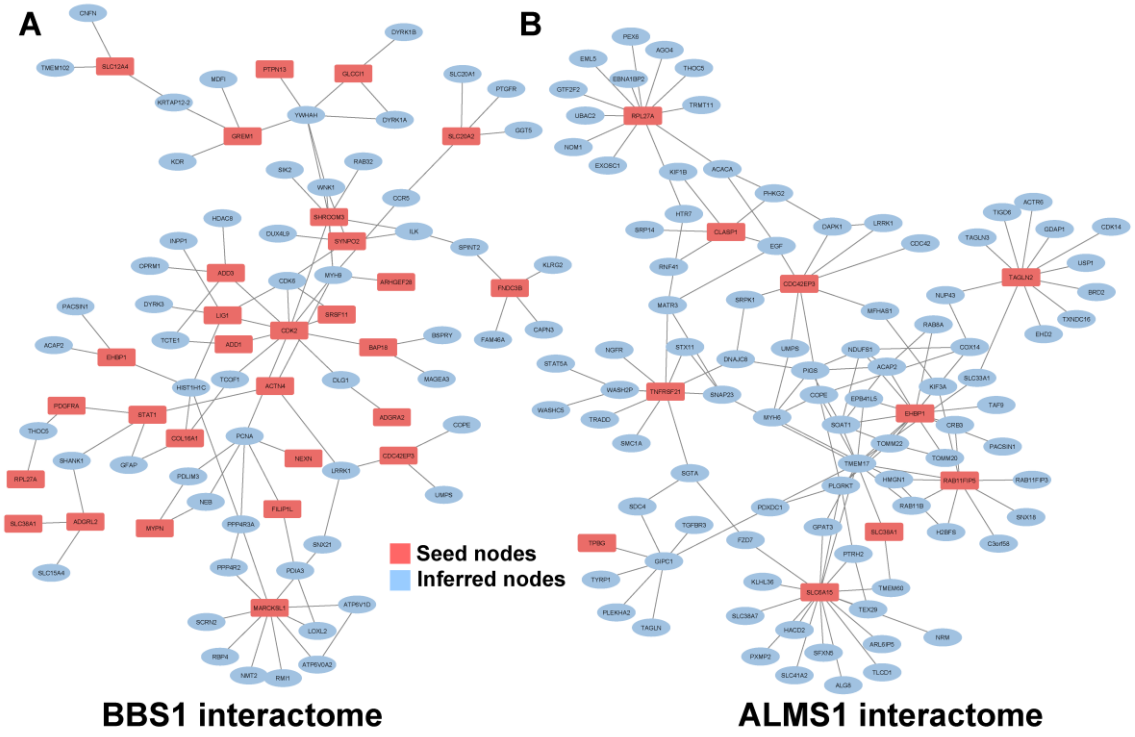

Figure 4. Protein-protein interaction analysis highlights CDK2 as the central node of the

BBS1 interactome and CDC42EP3 as the central node of the *ALMS1* interactome. Red nodes represent the DPP that were detected in the first analysis. Blue nodes represent the nodes inferred by RWR algorithm. **(A)** Interactome of the top 100 proteins with the highest RWR score after network diffusion in the *BBS1KO*. **(B)** Interactome of the top 100 proteins with the highest RWR score after network diffusion in the *ALMS1KO*.

Using the top 100 proteins with the highest RWR score, an analysis of protein-protein interactions was performed. In the case of *BBS1KO*, CDK2 (seed node), a key regulator of the cell cycle, was one of the most interconnected nodes, highlighting its central role in this interactome **(Figure 4A)**. On the other hand, in the case of *ALMS1KO*, CDC42EP3 a direct effector of CDC42, key regulator of cell cycle and migration processes, was found to be one of the most interconnected nodes in the network, highlighting its central role in the deregulated interactome of this model. It also highlights the highly interconnected cluster of RAB proteins such as RAB11 and RAB8A, resulted by EHBP1, that play an important role in endocytosis **(Figure 4B)**.

Kinase-substrate enrichment analysis uncovers CDK2 and CDC42 as the most phosphorylated substrates

To determine which DPP were subject to the highest level of up-regulation, a KSEA was performed with the top 100 with the highest RWR score. The proteins (substrates) subject to the highest level of up-regulation were again CDK2 in the case of *BBS1* and CDC42 in the case of *ALMS1* **(Figure 5A-B)**. The main kinases regulating the selected subset of proteins were AKT1 in *BBS1* and CDK2 in the case of *ALMS1* **(Figure 5A-B)**. This shows that the observed alterations have commonalities but appear to differ in their regulation.

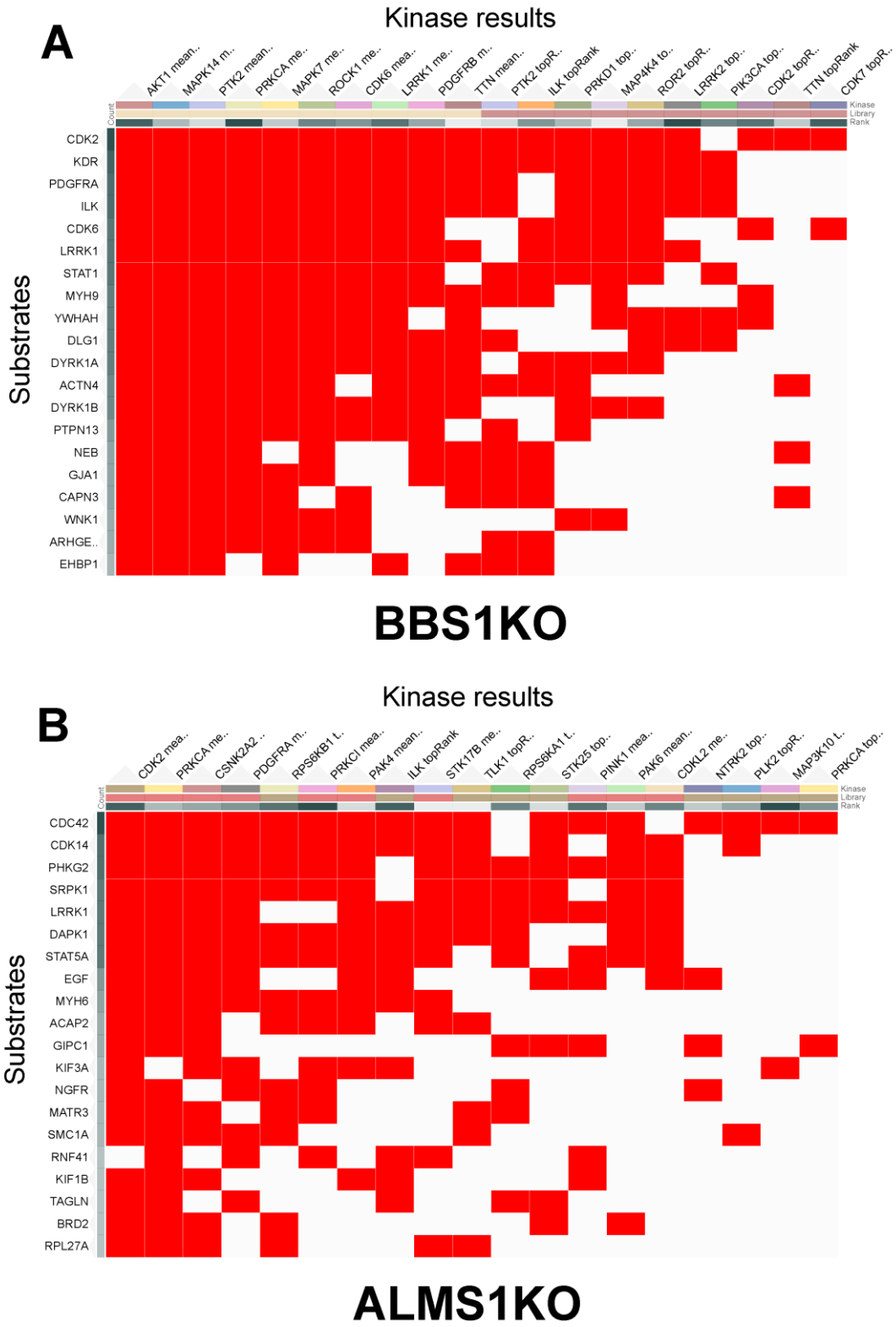

Figure 5. KSEA highlights CDK2 in *BBS1* and CDC42 in *ALMS1* as the main substrates subject to regulation. **(A)** KSEA of the top 100 proteins (substrates) with the highest RWR score after network diffusion in the *BBS1KO*. **(B)** KSEA of the top 100 proteins (substrates) with the highest RWR score after network diffusion in the *ALMS1KO*. The

299 plots only show the 20 most up-regulated proteins (substrates) out of the initial 100
300 proteins used in the analysis.

301 DISCUSSION

302 The TGF-β pathway is one of the main signalling pathways regulated by the primary
303 cilium (Clement et al., 2013; Pedersen et al., 2016; Christensen et al., 2017; Anvarian et
304 al., 2019). It controls processes related to cell proliferation and migration and is
305 associated with several pathologies such as liver or kidney fibrosis, recurrent
306 phenotypes in ciliopathies (Zhang et al., 2017; Guan et al., 2021; McConnachie et al.,
307 2021). Despite this, few studies have attempted to link ciliary gene dysfunction with
308 signalling alterations in the TGF-β pathway (Mönnich et al., 2018; Álvarez-Satta et al.,
309 2021; Bea-Mascato et al., 2022b, 2022a). In this study, we have applied
310 phosphoproteomics to determine alterations in the TGF-β signalling pathway in two
311 model ciliopathies, ALMS and BBS. We have further elucidated the regulation of the TGF-
312 β pathway in ALMS and established for the first time the link between the TGF-β
313 pathway and BBS genes (Álvarez-Satta et al., 2021; Bea-Mascato et al., 2022b, 2022a).

314 In this article, we designed and applied a pipeline that allowed us to obtain a global view
315 of the processes altered in the TGF-β pathway by inhibiting two ciliary genes, *ALMS1* and
316 *BBS1*. In the case of *ALMS1*, we found that the altered processes were mainly related to
317 endocytosis and mitosis (*via* the Syndecan 4 signalling pathway, responsible for
318 cytokinesis) (Keller-Pinter et al., 2010). The role of *ALMS1* in endocytotic and mitotic
319 processes has already been established in the past (Zulato et al., 2011; Collin et al., 2012;
320 Leitch et al., 2014; Jaykumar et al., 2018; Bea-Mascato et al., 2022b). However, this is
321 the first time that these alterations in endocytosis and mitosis could be related to the
322 TGF-β signalling pathway affecting the activation of RAB11FIP5 and EHBP1 (seed nodes)
323 and other related proteins such as RAB8A and RAB11B (inferred nodes) among others
324 (Rai et al., 2020; Solinger et al., 2020). In addition, the relationship of CDC42 in this
325 interactome has also been established through CDC42EP3, a CDC42 effector protein that
326 is under-phosphorylated in the differentially phosphorylated proteins detected in the
327 differential analysis **(Figures 4B, 2D)**. The significance of CDC42 has also been
328 determined by KSEA **(Figure 5B)**. CDC42 plays a key role in cell polarity and regulation of

329 mitosis (Witte et al., 2017; Moran et al., 2019; Rich-Robinson et al., 2021). CDC42EP3
330 acts downstream of CDC42 and regulates the rearrangement of the actin and septin
331 cytoskeleton (Farrugia and Calvo, 2016). Cell cycle disorders and cytoskeleton
332 alterations are common phenotypes in *ALMS1*-depleted cells, so a dysfunction of CDC42
333 and CDC42EP3 could be a possible cause of them (Zulato et al., 2011; Collin et al., 2012;
334 Shenje et al., 2014; Bea-Mascato et al., 2022b). Inhibition of CDC42EP3 and EHBP1 in
335 *BBS1*KO could indicate commonalities in regulation between *ALMS1* and *BBS1*, so that
336 the alterations detailed above could also be present when BBS1 is inhibited.

337 *BBS1* gene inhibition altered the phosphorylation of 41 proteins after TGF-β stimulation.
338 Following network diffusion, these proteins were found to be mainly involved in the
339 regulation of the extracellular matrix *via* the TGF-β pathway; cross-signalling with other
340 pathways such as p53, NOTCH1 or SHh and transport of cation ions (Ca^{2+} or Na^{+}) **(Figure**
341 **3B)**. Alterations of TGF-β signalling have already been described when inhibiting other
342 ciliary genes such as *ALMS1* or *CEP128*, but never for the *BBS1* gene (Mönnich et al.,
343 2018; Álvarez-Satta et al., 2021; Bea-Mascato et al., 2022b). Some of the main nodes of
344 the BBS1 interactome and KSEA were SYNPO2, CDK2 and PDGFRA proteins. SYNPO2,
345 which is over-phosphorylated, encodes actin binding proteins that has been
346 characterized as a tumor suppressor (OuYang et al., 2021). It is considered a protein with
347 inhibitory capacity on cell migration and proliferation (OuYang et al., 2021). On the
348 other hand, CDK2 and PDGFRA, which appear under-phosphorylated, are key regulators
349 of mitosis and cell proliferation (Elling et al., 2011; Spencer et al., 2013; Li et al., 2018).
350 Thus, the lack of BBS1 seems to prevent proper TGF-B-mediated proliferation. Our data
351 do not allow us to conclude the existence of a compensatory mechanism via another
352 pathway.

353 The main limitations of this study are related to the use of in vitro models, which often
354 do not fully reproduce patient phenotypes. For this reason, these results need to be
355 validated in primary samples or animal models to determine whether the alterations
356 described are conserved processes.

357 On the other hand, phosphoproteomics is an approach that allows the global analysis of
358 the activation of the cellular interactome. However, like any technique, it has several
359 limitations, since the phosphoproteome is estimated at 30% of the total proteome and

current enrichment techniques have a recovery of 1-3% of the total amount of starting sample (Low et al., 2021; Urban, 2022). The first limitation is due to a large amount of starting material needed to obtain the first data. The recommended starting material required is usually a minimum of 600µg-1mg of protein lysate (Solari et al., 2015). This is affordable when working with cell culture, but very complicated when working with tissue samples. This makes it necessary to develop techniques that increase the enrichment yield and allow the use of less starting material. Phosphoproteomics data are usually scarce and noisy, requiring the development of statistical techniques and analysis methodologies that allow robust inference from the data initially obtained (Solari et al., 2015). Furthermore, the nature of the data generated by current phosphoproteomics techniques introduces a bias in that kinases have only been identified from less than 5% of the phosphoproteome, and functional assignments of phosphosites are almost negligible (Needham et al., 2019).

CONCLUSION

In conclusion, the depletion of ciliary genes such as *ALMS1* and *BBS1* alters signal transduction through the TGF-β pathway, altering processes such as endocytosis and mitosis in the case of *ALMS1* and the regulation of the extracellular matrix, p53, NOTCH1, SHh and transport of cation ions in the case of *BBS1*. These phenomena could be explained by alterations affecting the inhibition of CDCD42 in the case of *ALMS1* or CDK2 in the case of *BBS1*.

Author Contributions: BB-M, DV designed the study. BB-M performed the experiments and analysis. EP led the design of the analysis pipeline for differential phosphorylation and network diffusion. GG and IP-S supervised and assisted in the analysis. CS performed the screening and characterisation of clones for the *BBS1* KO model. All authors wrote the manuscript and provided approval for publication.

Funding: This work was funded by Instituto de Salud Carlos III de Madrid FIS project PI15/00049 and PI19/00332, Xunta de Galicia (Centro de Investigación de Galicia CINBIO 2019-2022) Ref. ED431G-2019/06, Consolidación e estructuración de unidades de investigación competitivas e outras accións de fomento (ED431C-2018/54). Brais Bea-Mascato (FPU17/01567) and Carlos Solarat (FPU 19/00175) were supported by pre-

doctoral contracts (FPU predoctoral fellowships) from the Spanish Ministry of Education, Culture and Sports. Brais Bea-Mascato was also supported by an EMBL Corporate Partnership Programme Scientific Visitors Fellowship.

Informed Consent Statement: Not Apply.

Data Availability Statement: Data are available via ProteomeXchange with the identifier PXD037573.

Code Availability Statement: The code used in this study can be consulted on the GitHub repository https://github.com/BreisOne/phosphoproteome_pipeline.

Acknowledgements: We sincerely thank the Proteomics and Genomics services from Centro de Apoyo Científico-Tecnológico a la Investigación (CACTI) of University of Vigo and its specialists Paula Álvarez Chaver, Ángel Sebastián Comesaña, Verónica Outeiriño and Manuel Marcos for their guidance and advise. We also thank Mercedes Peleteiro Olmedo from Centro de Investigacións Biomédicas (CINBIO) from University of Vigo for the flow cytometry service. Finally, thanks to Eduard Sabido and Cristina Chiva Rodríguez from the Centre for Genomic Regulation (CRG) of the Pompeu Fabra University (UPF) for the data acquisition service and their advice and guidance in optimising the process.

Conflicts of Interest: The authors declare no conflict of interest. The funders had no role in the design of the study; in the collection, analyses, or interpretation of data; in the writing of the manuscript, or in the decision to publish the results.

REFERENCES:

Aliferis, K., Hellé, S., Gyapay, G., Duchatelet, S., Stoetzel, C., Mandel, J. L., et al. (2012). Differentiating Alström from Bardet-Biedl syndrome (BBS) using systematic ciliopathy genes sequencing. *Ophthalmic Genet.* 33, 18–22. doi: 10.3109/13816810.2011.620055.

Álvarez-Satta, M., Lago-Docampo, M., Bea-Mascato, B., Solarat, C., Castro-Sánchez, S., Christensen, S. T., et al. (2021). ALMS1 Regulates TGF-β Signaling and Morphology of Primary Cilia. *Front. Cell Dev. Biol.* 9, 112. doi: 10.3389/fcell.2021.623829.

Anvarian, Z., Mykytyn, K., Mukhopadhyay, S., Pedersen, L. B., and Christensen, S. T. (2019). Cellular signalling by primary cilia in development, organ function and disease. *Nat. Rev. Nephrol.* 15, 199–219. doi: 10.1038/s41581-019-0116-9.

Baig, S., Paisey, R., Dawson, C., Barrett, T., Maffei, P., Hodson, J., et al. (2020). Defining renal phenotype in Alström syndrome. *Nephrol. Dial. Transplant* 35, 994–1001. doi: 10.1093/ndt/gfy293.

Bea-Mascato, B., Gómez-Castañeda, E., Sánchez-Corrales, Y. E., Castellano, S., and Valverde, D. (2022a). Loss of the centrosomal protein ALMS1 alters lipid metabolism and the regulation of extracellular matrix-related processes. *bioRxiv*, 2022.11.02.514847. doi: 10.1101/2022.11.02.514847.

Bea-Mascato, B., Neira-Goyanes, E., Iglesias-Rodríguez, A., and Valverde, D. (2022b). Depletion of ALMS1 affects TGF-β signalling pathway and downstream processes such as cell migration and adhesion capacity. *Front. Mol. Biosci.* 9, 1085. doi: 10.3389/fmolb.2022.992313.

Berbari, N. F., O'Connor, A. K., Haycraft, C. J., and Yoder, B. K. (2009). The Primary Cilium as a Complex Signaling Center. *Curr. Biol.* 19, R526–R535. doi: 10.1016/J.CUB.2009.05.025.

Christensen, S. T., Clement, C. A., Satir, P., and Pedersen, L. B. (2012). Primary cilia and coordination of receptor tyrosine kinase (RTK) signalling. *J. Pathol.* 226, 172–184. doi: 10.1002/path.3004.

437 Christensen, S. T., Morthorst, S. K., Mogensen, J. B., and Pedersen, L. B. (2017). Primary
438 Cilia and Coordination of Receptor Tyrosine Kinase (RTK) and Transforming Growth
439 Factor β (TGF-β) Signaling. *Cold Spring Harb. Perspect. Biol.* 9, a028167. doi:
440 10.1101/CSHPERSPECT.A028167.

441 Clement, C. A., Ajbro, K. D., Koefoed, K., Vestergaard, M. L., Veland, I. R., Henriques de
442 Jesus, M. P. R., et al. (2013). TGF-β signaling is associated with endocytosis at the
443 pocket region of the primary cilium. *Cell Rep.* 3, 1806–14. doi:
444 10.1016/j.celrep.2013.05.020.

445 Collin, G. B., Marshall, J. D., Ikeda, A., So, W. V., Russell-Eggitt, I., Maffei, P., et al. (2002).
446 Mutations in ALMS1 cause obesity, type 2 diabetes and neurosensory degeneration
447 in Alström syndrome. *Nat. Genet.* 31, 74–8. doi: 10.1038/ng867.

448 Collin, G. B., Marshall, J. D., King, B. L., Milan, G., Maffei, P., Jagger, D. J., et al. (2012).
449 The Alström syndrome protein, ALMS1, interacts with α-actinin and components of
450 the endosome recycling pathway. *PLoS One* 7, e37925–e37925. doi:
451 10.1371/journal.pone.0037925.

452 Csardi, G., and Nepusz, T. (2006). The igraph software package for complex network
453 research. *InterJournal, complex Syst.* 1695, 1–9.

454 Elling, C., Erben, P., Walz, C., Frickenhaus, M., Schemionek, M., Stehling, M., et al. (2011).
455 Novel imatinib-sensitive PDGFRA-activating point mutations in hypereosinophilic
456 syndrome induce growth factor independence and leukemia-like disease. *Blood*
457 117, 2935–2943. doi: 10.1182/BLOOD-2010-05-286757.

458 Farrugia, A. J., and Calvo, F. (2016). Cdc42 regulates Cdc42EP3 function in cancer-
459 associated fibroblasts. *http://dx.doi.org/10.1080/21541248.2016.1194952* 8, 49–
460 57. doi: 10.1080/21541248.2016.1194952.

461 Finnson, K. W., Almadani, Y., and Philip, A. (2020). Non-canonical (non-SMAD2/3) TGF-β
462 signaling in fibrosis: Mechanisms and targets. *Semin. Cell Dev. Biol.* 101, 115–122.
463 doi: 10.1016/J.SEMCDB.2019.11.013.

464 Forsythe, E., and Beales, P. L. (2012). Bardet–Biedl syndrome. *Eur. J. Hum. Genet. 2013*
465 *211* 21, 8–13. doi: 10.1038/ejhg.2012.115.

466 Forsythe, E., Kenny, J., Bacchelli, C., and Beales, P. L. (2018). Managing Bardet-Biedl
467 syndrome-now and in the future. *Front. Pediatr.* 6, 23. doi:
468 10.3389/FPED.2018.00023/XML/NLM.

469 Gasior, K., Wagner, N. J., Cores, J., Caspar, R., Wilson, A., Bhattacharya, S., et al. (2019).
470 The role of cellular contact and TGF-beta signaling in the activation of the epithelial
471 mesenchymal transition (EMT). *Cell Adhes. Migr.* 13, 63–75. doi:
472 10.1080/19336918.2018.1526597.

473 Gerdes, J. M., Davis, E. E., and Katsanis, N. (2009). The Vertebrate Primary Cilium in
474 Development, Homeostasis, and Disease. *Cell* 137, 32. doi:
475 10.1016/J.CELL.2009.03.023.

476 Guan, Y., Enejder, A., Wang, M., Fang, Z., Cui, L., Chen, S. Y., et al. (2021). A human multi-
477 lineage hepatic organoid model for liver fibrosis. *Nat. Commun. 2021 121* 12, 1–15.
478 doi: 10.1038/s41467-021-26410-9.

479 Hamidi, A., Song, J., Thakur, N., Itoh, S., Marcusson, A., Bergh, A., et al. (2017). TGF-β
480 promotes PI3K-AKT signaling and prostate cancer cell migration through the TRAF6-
481 mediated ubiquitylation of p85α. *Sci. Signal.* 10. doi: 10.1126/SCISIGNAL.AAL4186.

482 Harispe, S., Ranwez, S., Janaqi, S., and Montmain, J. (2014). The semantic measures
483 library and toolkit: Fast computation of semantic similarity and relatedness using
484 biomedical ontologies. *Bioinformatics* 30, 740–742. doi:
485 10.1093/bioinformatics/btt581.

486 Hearn, T. (2018). ALMS1 and Alström syndrome: a recessive form of metabolic,
487 neurosensory and cardiac deficits. *J. Mol. Med.* doi: 10.1007/s00109-018-1714-x.

488 Hearn, T., Spalluto, C., Phillips, V. J., Renforth, G. L., Copin, N., Hanley, N. A., et al. (2005).
489 Subcellular Localization of ALMS1 Supports Involvement of Centrosome and Basal
490 Body Dysfunction in the Pathogenesis of Obesity, Insulin Resistance, and Type 2
491 Diabetes. *Diabetes* 54, 1581 LP – 1587. doi: 10.2337/diabetes.54.5.1581.

492 Ishikawa, H., and Marshall, W. F. (2011). Ciliogenesis: building the cell's antenna. *Nat.*
493 *Rev. Mol. Cell Biol.* 12, 222–234. doi: 10.1038/NRM3085.

494 Jain, S., and Bader, G. D. (2010). An improved method for scoring protein-protein
495 interactions using semantic similarity within the gene ontology. *BMC*
496 *Bioinformatics* 11, 562. doi: 10.1186/1471-2105-11-562.

497 Jaykumar, A. B., Caceres, P. S., King-Medina, K. N., Liao, T.-D., Datta, I., Maskey, D., et al.
498 (2018). Role of Alström syndrome 1 in the regulation of blood pressure and renal
499 function. *JCI insight* 3, e95076. doi: 10.1172/jci.insight.95076.

500 Keller-Pinter, A., Bottka, S., Timar, J., Kulka, J., Katona, R., Dux, L., et al. (2010). Syndecan-
501 4 promotes cytokinesis in a phosphorylation-dependent manner. *Cell. Mol. Life Sci.*
502 67, 1881–94. doi: 10.1007/s00018-010-0298-6.

503 Klink, B. U., Gatsogiannis, C., Hofnagel, O., Wittinghofer, A., and Raunser, S. (2020).
504 Structure of the human BBSome core complex. *Elife* 9. doi: 10.7554/ELIFE.53910.

505 Köhler, S., Bauer, S., Horn, D., and Robinson, P. N. (2008). Walking the Interactome for
506 Prioritization of Candidate Disease Genes. *Am. J. Hum. Genet.* 82, 949–958. doi:
507 10.1016/j.ajhg.2008.02.013.

508 Kuleshov, M. V., Jones, M. R., Rouillard, A. D., Fernandez, N. F., Duan, Q., Wang, Z., et al.
509 (2016). Enrichr: a comprehensive gene set enrichment analysis web server 2016
510 update. *Nucleic Acids Res.* 44, W90. doi: 10.1093/NAR/GKW377.

511 Kuleshov, M. V, Xie, Z., London, A. B. K., Yang, J., Evangelista, J. E., Lachmann, A., et al.
512 (2021). KEA3: improved kinase enrichment analysis via data integration. *Nucleic*
513 *Acids Res.* 49, W304–W316. doi: 10.1093/nar/gkab359.

514 Lan, H. Y. (2011). Diverse roles of TGF-β/Smads in renal fibrosis and inflammation. *Int. J.*
515 *Biol. Sci.* 7, 1056–1067. doi: 10.7150/IJBS.7.1056.

516 Leitch, C. C., Lodh, S., Prieto-Echagüe, V., Badano, J. L., and Zaghloul, N. A. (2014). Basal
517 body proteins regulate Notch signaling through endosomal trafficking. *J. Cell Sci.*
518 127, 2407–19. doi: 10.1242/jcs.130344.

519 Li, G., Vega, R., Nelms, K., Gekakis, N., Goodnow, C., McNamara, P., et al. (2007). A role
520 for Alström syndrome protein, alms1, in kidney ciliogenesis and cellular quiescence.
521 *PLoS Genet.* 3, e8. doi: 10.1371/journal.pgen.0030008.

522 Li, R., Bernau, K., Sandbo, N., Gu, J., Preissl, S., and Sun, X. (2018). Pdgfra marks a cellular
523 lineage with distinct contributions to myofibroblasts in lung maturation and injury
524 response. *Elife* 7. doi: 10.7554/ELIFE.36865.

525 Licata, L., Lo Surdo, P., Iannuccelli, M., Palma, A., Micarelli, E., Perfetto, L., et al. (2020).
526 SIGNOR 2.0, the SIGnaling Network Open Resource 2.0: 2019 update. *Nucleic Acids*
527 *Res.* 48, D504–D510. doi: 10.1093/nar/gkz949.

528 Low, T. Y., Mohtar, M. A., Lee, P. Y., Omar, N., Zhou, H., and Ye, M. (2021). Widening the
529 bottleneck of phosphoproteomics: evolving strategies for phosphopeptide
530 enrichment. *Mass Spectrom. Rev.* 40, 309–333. doi: 10.1002/mas.21636.

531 Luo, K. (2017). Signaling Cross Talk between TGF-β/Smad and Other Signaling Pathways.
532 *Cold Spring Harb. Perspect. Biol.* 9, a022137. doi: 10.1101/cshperspect.a022137.

533 Marshall, J. D., Maffei, P., Collin, G. B., and Naggert, J. K. (2011). Alström syndrome:
534 genetics and clinical overview. *Curr. Genomics* 12, 225–235. doi:
535 10.2174/138920211795677912.

536 Massagué, J. (2012). TGFβ signalling in context. *Nat. Rev. Mol. Cell Biol.* 13, 616–630.
537 doi: 10.1038/nrm3434.

538 May-Simera, H. L., Wan, Q., Jha, B. S., Hartford, J., Khristov, V., Dejene, R., et al. (2018).
539 Primary Cilium-Mediated Retinal Pigment Epithelium Maturation Is Disrupted in
540 Ciliopathy Patient Cells. *Cell Rep.* 22, 189–205. doi: 10.1016/j.celrep.2017.12.038.

541 McConnachie, D. J., Stow, J. L., and Mallett, A. J. (2021). Ciliopathies and the Kidney: A
542 Review. *Am. J. Kidney Dis.* 77, 410–419. doi: 10.1053/J.AJKD.2020.08.012.

543 Meng, X. M., Nikolic-Paterson, D. J., and Lan, H. Y. (2014). Inflammatory processes in
544 renal fibrosis. *Nat. Rev. Nephrol. 2014 109* 10, 493–503. doi:
545 10.1038/nrneph.2014.114.

546 Meyer, J. R., Krentz, A. D., Berg, R. L., Richardson, J. G., Pomeroy, J., Hebbring, S. J., et al.
547 (2022). Kidney failure in Bardet–Biedl syndrome. *Clin. Genet.* 101, 429–441. doi:
548 10.1111/CGE.14119.

549 Mönnich, M., Borgeskov, L., Breslin, L., Jakobsen, L., Rogowski, M., Doganli, C., et al.

550 (2018). CEP128 Localizes to the Subdistal Appendages of the Mother Centriole and
551 Regulates TGF-β/BMP Signaling at the Primary Cilium. *Cell Rep.* 22, 2584–2592. doi:
552 10.1016/J.CELREP.2018.02.043.

553 Moran, K. D., Kang, H., Araujo, A. V., Zyla, T. R., Saito, K., Tsygankov, D., et al. (2019).
554 Cell-cycle control of cell polarity in yeast. *J. Cell Biol.* 218, 171–189. doi:
555 10.1083/JCB.201806196.

556 Needham, E. J., Parker, B. L., Burykin, T., James, D. E., and Humphrey, S. J. (2019).
557 Illuminating the dark phosphoproteome. *Sci. Signal.* 12. doi:
558 10.1126/scisignal.aau8645.

559 Orchard, S., Ammari, M., Aranda, B., Breuza, L., Briganti, L., Broackes-Carter, F., et al.
560 (2014). The MIntAct project—IntAct as a common curation platform for 11
561 molecular interaction databases. *Nucleic Acids Res.* 42, D358–D363. doi:
562 10.1093/NAR/GKT1115.

563 OuYang, C., Xie, Y., Fu, Q., and Xu, G. (2021). SYNPO2 suppresses hypoxia-induced
564 proliferation and migration of colorectal cancer cells by regulating YAP-KLF5 axis.
565 *Tissue Cell* 73, 101598. doi: https://doi.org/10.1016/j.tice.2021.101598.

566 Pedersen, L. B., Mogensen, J. B., and Christensen, S. T. (2016). Endocytic Control of
567 Cellular Signaling at the Primary Cilium. *Trends Biochem. Sci.* 41, 784–797. doi:
568 10.1016/J.TIBS.2016.06.002.

569 Perea-Romero, I., Solarat, C., Blanco-Kelly, F., Sanchez-Navarro, I., Bea-Mascato, B.,
570 Martin-Salazar, E., et al. (2022). Allelic overload and its clinical modifier effect in
571 Bardet-Biedl syndrome. *npj Genomic Med.* 7, 1–7. doi: 10.1038/s41525-022-00311-
572 2.

573 Putoux, A., Attie-Bitach, T., Martinovic, J., and Gubler, M. C. (2012). Phenotypic
574 variability of Bardet-Biedl syndrome: Focusing on the kidney. *Pediatr. Nephrol.* 27,
575 7–15. doi: 10.1007/S00467-010-1751-3/TABLES/2.

576 Rai, A., Bleimling, N., Vetter, I. R., and Goody, R. S. (2020). The mechanism of activation
577 of the actin binding protein EHBP1 by Rab8 family members. *Nat. Commun.* 11,
578 4187. doi: 10.1038/s41467-020-17792-3.

579 Reiter, J. F., and Leroux, M. R. (2017). Genes and molecular pathways underpinning
580 ciliopathies. *Nat. Rev. Mol. Cell Biol.* 18, 533–547. doi: 10.1038/nrm.2017.60.

581 Rich-Robinson, J., Russell, A., Mancini, E., and Das, M. (2021). Cdc42 reactivation at
582 growth sites is regulated by local cell-cycle-dependent loss of its GTPase-activating
583 protein Rga4 in fission yeast. *J. Cell Sci.* 134. doi: 10.1242/JCS.259291.

584 Shannon, P., Markiel, A., Ozier, O., Baliga, N. S., Wang, J. T., Ramage, D., et al. (2003).
585 Cytoscape: A Software Environment for Integrated Models of Biomolecular
586 Interaction Networks. *Genome Res.* 13, 2498–2504. doi: 10.1101/GR.1239303.

587 Shenje, L. T., Andersen, P., Halushka, M. K., Lui, C., Fernandez, L., Collin, G. B., et al.
588 (2014). Mutations in Alström protein impair terminal differentiation of
589 cardiomyocytes. *Nat. Commun.* 5, 3416. doi: 10.1038/ncomms4416.

590 Singh, S., Gui, M., Koh, F., Yip, M. C. J., and Brown, A. (2020). Structure and activation
591 mechanism of the BBSome membrane protein trafficking complex. *Elife* 9. doi:
592 10.7554/ELIFE.53322.

593 Solari, F. A., Dell'Aica, M., Sickmann, A., and Zahedi, R. P. (2015). Why
594 phosphoproteomics is still a challenge. *Mol. Biosyst.* 11, 1487–1493. doi:
595 10.1039/c5mb00024f.

596 Solinger, J. A., Rashid, H.-O., Prescianotto-Baschong, C., and Spang, A. (2020). FERARI is
597 required for Rab11-dependent endocytic recycling. *Nat. Cell Biol.* 22, 213–224. doi:
598 10.1038/s41556-019-0456-5.

599 Spencer, S. L., Cappell, S. D., Tsai, F. C., Overton, K. W., Wang, C. L., and Meyer, T. (2013).
600 The Proliferation-Quiescence Decision Is Controlled by a Bifurcation in CDK2
601 Activity at Mitotic Exit. *Cell* 155, 369–383. doi: 10.1016/J.CELL.2013.08.062.

602 Tong, H., Faloutsos, C., and Pan, J. (2006). Fast Random Walk with Restart and Its
603 Applications. in *Sixth International Conference on Data Mining (ICDM'06)*, 613–622.
604 doi: 10.1109/ICDM.2006.70.

605 Türei, D., Korcsmáros, T., and Saez-Rodriguez, J. (2016). OmniPath: Guidelines and
606 gateway for literature-curated signaling pathway resources. *Nat. Methods* 13, 966–

607 967. doi: 10.1038/nmeth.4077.

608 Urban, J. (2022). A review on recent trends in the phosphoproteomics workflow. From
609 sample preparation to data analysis. *Anal. Chim. Acta* 1199, 338857. doi:
610 10.1016/J.ACA.2021.338857.

611 Waldman, M., Han, J. C., Reyes-Capo, D. P., Bryant, J., Carson, K. A., Turkbey, B., et al.
612 (2018). Alström syndrome: Renal findings in correlation with obesity, insulin
613 resistance, dyslipidemia and cardiomyopathy in 38 patients prospectively
614 evaluated at the NIH clinical center. *Mol. Genet. Metab.* 125, 181–191. doi:
615 10.1016/j.ymgme.2018.07.010.

616 Waters, A. M., and Beales, P. L. (2011). Ciliopathies: An expanding disease spectrum.
617 *Pediatr. Nephrol.* 26, 1039–1056. doi: 10.1007/S00467-010-1731-7/FIGURES/5.

618 Witte, K., Strickland, D., and Glotzer, M. (2017). Cell cycle entry triggers a switch
619 between two modes of Cdc42 activation during yeast polarization. *Elife* 6. doi:
620 10.7554/ELIFE.26722.

621 Zhang, X., Smits, A. H., van Tilburg, G. B., Ovaa, H., Huber, W., and Vermeulen, M. (2018).
622 Proteome-wide identification of ubiquitin interactions using UbIA-MS. *Nat. Protoc.*
623 13, 530–550. doi: 10.1038/nprot.2017.147.

624 Zhang, Y., Alexander, P. B., and Wang, X. F. (2017). TGF-β family signaling in the control
625 of cell proliferation and survival. *Cold Spring Harb. Perspect. Biol.* 9. doi:
626 10.1101/cshperspect.a022145.

627 Zulato, E., Favaretto, F., Veronese, C., Campanaro, S., Marshall, J. D., Romano, S., et al.
628 (2011). ALMS1-deficient fibroblasts over-express extra-cellular matrix components,
629 display cell cycle delay and are resistant to apoptosis. *PLoS One* 6, e19081–e19081.
630 doi: 10.1371/journal.pone.0019081.

631